

# Scattering and Absorption of Waves by Flat Material Strips Analyzed Using Generalized Boundary Conditions and Nystrom-Type Algorithm

Olga V. Shapoval, *Student Member, IEEE*, Ronan Sauleau, *Senior Member, IEEE*, and Alexander I. Nosich, *Fellow, IEEE*

**Abstract**—The scattering of the H- and E-polarized plane waves by a thin flat homogeneous magneto-dielectric strip is considered. Assuming the strip to be thinner than the wavelength, we shrink its cross-section to the median line where the generalized boundary conditions are imposed. The numerical solution is built on two singular integral equations discretized using Nystrom-type numerical algorithm. The obtained results demonstrate fast convergence and good agreement with data known for the limiting values of the strip parameters. This opens a way to the accurate numerical analysis of various striplike configurations simulating natural objects and electromagnetic circuit components, both in traditional microwave applications and nanophotonics.

**Index Terms**—Discrete mathematical model, generalized two-side boundary conditions, scattering cross-sections, singular and hyper-singular integral equations, strip scatterer.

## I. INTRODUCTION

STRIPS and striplike scatterers are frequently met in microwave and photonic devices because of their simple manufacturing with the existing etching and printing technologies. Their thickness usually makes a fraction of the free-space electromagnetic wave length while the width can be smaller, comparable to and larger than the wavelength. This combination of parameters makes both quasistatic and high-frequency methods of analysis inapplicable and thus the full-wave methods are mandatory. Still the small thickness suggests that the analysis can be simplified by neglecting the internal field of the strip and considering only the limiting values of the field components. Materials of such scatterers vary greatly, and so vary their theoretical models, from perfect electrically conducting (PEC) to resistive

and impedance strips. In the optical range, the model of PEC scatterer is not applicable at all, even for the scatterers made of the noble metals like gold and silver. All mentioned dictates a necessity of the development of new accurate mathematical models and convergent numerical methods for the scattering by the thin magneto-dielectric strips.

In this paper, the two-dimensional (2-D) electromagnetic wave scattering and absorption by a flat material strip is characterized using the two-side generalized boundary conditions (GBC) and singular integral equations (IEs) [1]. The novelty of the paper is, first, in the use of the special type of GBC proposed in [2]–[4], valid for a thin and high-contrast material layer. This is unlike the important earlier studies [5]–[8], where a small material contrast was implied. Second, to solve the IEs we develop a fast and convergent Nystrom-type numerical algorithm having controlled accuracy.

There are many techniques for building the numerical solutions to the IEs in the 2-D scattering by the striplike structures including PEC and imperfect strips, e.g., dielectric and impedance, both stand-alone and periodically structured: the Galerkin moment method [9], the inverse Fourier transform method [10], and, apparently the most advantageous, the method of analytical regularization [11]–[17]. The last of the mentioned guarantees convergence of numerical solutions and provides 3–4 digit accuracy with a relatively small number of unknowns. Besides, recently the Nystrom-type numerical techniques using the quadratures and interpolation-based discretization have attracted attention of researchers [18]–[23]. They have been already demonstrated as convergent, economic and simple in implementation for the modeling of the scattering by PEC zero-thickness flat and curved strips [20]–[27]. Therefore here we are going to extend them to the analysis of stand-alone imperfect flat strips.

The paper is organized as follows. In Section II, we formulate the plane-wave scattering problem for a thin material (magneto-dielectric) flat strip using GBS and obtain the basic IEs. Section III describes details of the proposed Nystrom-type numerical algorithm. In Section IV, we demonstrate and discuss the numerical results for various strips. Conclusions are summarized in Section V.

## II. FORMULATION AND BASIC EQUATIONS

### A. Formulation

Consider the 2-D scattering problem for a magneto-dielectric strip of the width  $d$  and thickness  $h$ , characterized with the

Manuscript received July 22, 2010; revised December 24, 2010; accepted February 23, 2011. Date of publication July 12, 2011; date of current version September 02, 2011. This work was supported in part by the National Academy of Sciences of Ukraine in the framework of Target Program “Nanotechnologies and Nanomaterials,” the State Committee for Science, Ukraine via the project M/146-2009, and in part by the European Science Foundation via research network project “Newfocus.” The work of O. V. Shapoval was supported by a Doctoral Research Award from the IEEE Antennas and Propagation Society.

O. V. Shapoval is with the Institute of Radio-Physics and Electronics, National Academy of Sciences of Ukraine, Kharkiv 61085, Ukraine (e-mail: olga.v.shapoval@gmail.com).

R. Sauleau is with the Institute of Electronics and Telecommunications of Rennes, Université de Rennes 1, 35042 Rennes, France

A. I. Nosich is with the Institute of Radio-Physics and Electronics, National Academy of Sciences of Ukraine, Kharkiv 61085, Ukraine and also with the Université Européenne de Bretagne, c/o Université de Rennes 1, Rennes Cedex 35042, France.

Color versions of one or more of the figures in this paper are available online at <http://ieeexplore.ieee.org>.

Digital Object Identifier 10.1109/TAP.2011.2161547

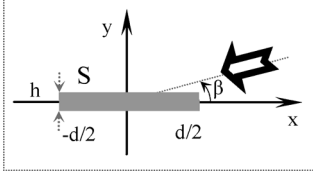


Fig. 1. Geometry of the problem.

relative material constants  $\epsilon_r$  and  $\mu_r$ . Suppose that the strip is illuminated by an H-polarized electromagnetic plane wave incident at the angle  $\beta$  measured from the  $x$ -axis (Fig. 1). The time factor is assumed as  $e^{-i\omega t}$  and omitted.

The total magnetic field has only  $z$ -component, which can be represented as a sum,  $u_{tot}(\vec{r}) = u_{sc}(\vec{r}) + u_0(\vec{r})$ , where  $u_0(\vec{r}) = e^{-ik(x \cos \beta + y \sin \beta)}$  is the incident plane wave ( $k$  being the free-space wavenumber) and  $u_{sc}(\vec{r})$  is the scattered field.

Outside of the strip surface the total field is required to satisfy the Helmholtz equation. Assuming that the strip is thin, we follow [2]–[4], replace the strip cross-section with its central line,  $S = \{(x, y) : |x| < d/2, y = 0\}$ , and impose, on  $S$ , the following two-side generalized boundary conditions,

$$\frac{\partial}{\partial \vec{n}} [u_{tot}^+(\vec{r}) + u_{tot}^-(\vec{r})] = -2ikR[u_{tot}^+(\vec{r}) - u_{tot}^-(\vec{r})] \quad (1)$$

$$[u_{tot}^+(\vec{r}) + u_{tot}^-(\vec{r})] = \frac{2iQ}{k} \frac{\partial}{\partial \vec{n}} [u_{tot}^+(\vec{r}) - u_{tot}^-(\vec{r})] \quad (2)$$

where  $\vec{n}$  is the one-side unit normal vector on  $S$ .

Note that such GBC appear provided that two sides of the strip have identical properties. They allow us to eliminate from consideration the field inside the strip. This is done at the expense of introducing the so-called relative electric and magnetic resistivities,  $R$  and  $Q$ . Note also that PEC boundary conditions follow from (1) and (2) if  $R = 0$  and  $|Q| = \infty$ . In the case of E-polarization, the function  $u(\vec{r})$  should be understood as the electric field  $z$ -component and the values  $R$  and  $Q$  in (1) and (2) exchange their places. Additionally,  $u_{sc}(x, y)$  must satisfy Sommerfeld radiation condition at infinity and condition of the local energy finiteness in any finite domain enclosing an edge point. This scattering problem is uniquely solvable (see [1]).

### B. Resistivities

According to three independent derivations [2]–[4] that are in agreement with each other, relative electric and magnetic resistivities of a thin homogeneous material layer are found as

$$R = \frac{iZ_r}{2} \cot\left(\frac{kh\sqrt{\epsilon_r\mu_r}}{2}\right), \quad Q = \frac{i}{2Z_r} \cot\left(\frac{kh\sqrt{\epsilon_r\mu_r}}{2}\right) \quad (3)$$

where  $Z_r = (\mu_r/\epsilon_r)^{1/2}$  is the relative material impedance. The formulas (3) are valid under the conditions that  $kh \ll 1$  and  $|\epsilon_r\mu_r| \gg 1$ , i.e., a high contrast is implied [3]. This is important difference from the model used in [5]–[8] that required a small contrast,  $|kh\epsilon_r - 1| \ll 1$ . Note that  $R$  and  $Q$  can, in principle, be the functions of  $x$ .

### C. Singular Integral Equations

We assume that in the case of arbitrary H-polarized (or E-polarized) incident wave the solution of the problem can be found as a sum of the single-layer and double-layer potentials

$$u_{sc}(\vec{r}) = \frac{ik}{4} \int_S V(\vec{r}') H_0^{(1)}(k|\vec{r} - \vec{r}'|) d\vec{r}' + \frac{i}{4} \int_S W(\vec{r}') \frac{\partial H_0^{(1)}(k|\vec{r} - \vec{r}'|)}{\partial \vec{n}(\vec{r}')} d\vec{r}' \quad (4)$$

where  $H_0^{(1)}(\cdot)$  is the Hankel function, and  $V(\vec{r})$  and  $W(\vec{r})$  are the unknown surface currents of magnetic and electric type induced on the strip. It is obvious from the characteristics of the potentials that thus defined function satisfies Helmholtz equation off  $S$  and the referred above radiation condition.

Using GBC and the properties of the limit values of potentials when crossing the integration contour, we reduce our problem to two decoupled IEs (see also [4], [7]) with logarithmic-type and hyper-type singularities, respectively

$$4QV(x_0) + k \int_{-d/2}^{+d/2} V(x) H_0^{(1)}(k|x - x_0|) dx = 4ie^{-ikx_0 \cos \beta} \quad (5)$$

$$4RW(x_0) + \int_{-d/2}^{+d/2} W(x) \frac{H_1^{(1)}(k|x - x_0|)}{|x - x_0|} dx = 4 \sin \beta e^{-ikx_0 \cos \beta} \quad (6)$$

where  $x_0 \in (-d/2, d/2)$ . Note that in the case of the E-polarization the scattering problem is reduced to two IEs like (5) and (6) where  $R$  and  $Q$  exchange their places.

## III. DISCRETE MODEL OF THE PROBLEM

### A. Discretization Using the Quadratures

Introduce dimensionless value  $\kappa = kd/2$  and unknown function  $\tilde{W}(x) = W(x)/\sqrt{(1/2 - x/d)(1/2 + x/d)}$ , and change the variable to  $t = 2x/d$ ,  $t \in [-1, 1]$ . Then the IEs take form as

$$4QV(t_0) + \kappa \int_{-1}^1 V(t) H_0^{(1)}(\kappa|t - t_0|) dt = 4e^{-i\kappa t_0 \cos \beta} \quad (7)$$

$$4R\tilde{W}(t_0) \sqrt{1 - t_0^2} + \int_{-1}^1 \tilde{W}(t) \sqrt{1 - t^2} \frac{H_1^{(1)}(\kappa|t - t_0|)}{|t - t_0|} dt = 8 \sin \beta e^{-i\kappa t_0 \cos \beta}. \quad (8)$$

The principal terms of the asymptotic expansions of the Hankel functions at  $z \rightarrow 0$  are given by  $H_0^{(1)}(z) \sim 2i \ln(z/2)/\pi$  and  $H_1^{(1)}(z)/z \sim (i/\pi) \ln z - 2i/(\pi z^2)$ , respectively. Hence, the kernel functions of (7) and (8) can be presented as

$$H_0^{(1)}(k|t - t_0|) = \left(\frac{2i}{\pi}\right) \ln |t - t_0| + M_0(t, k) \quad (9)$$

$$\frac{H_1^{(1)}(k|t - t_0|)}{|t - t_0|} = \frac{ik \ln |t - t_0|}{\pi} - \frac{2i}{\pi k |t - t_0|^2} + N_0(t, k) \quad (10)$$

where  $M_0(t, k)$  and  $N_0(t, k)$  are smooth functions.

Therefore, the hyper-singular integral in (8) is understood in the sense of finite part by Hadamard.

For the discretization of (7) we use the Simpson quadrature formulas (see [28]) with the equidistant grid  $\tau_j^m, j = 1, 2, \dots, m$  after performing the transformation,

$$\int_0^1 V(t) \ln |t - t_0| dt = \int_0^1 [V(t) - V(t_0)] \ln |t - t_0| dt + V(t_0) \xi(t_0) \quad (11)$$

where  $\xi(t_0) = t_0 \ln t_0 + (1 - t_0) \ln(1 - t_0) - 1$ . For IE (8), we use quadrature formulas of interpolation type (see [19]) with the nodes at  $t_{0j}^n = \cos(\pi j/n), j = 1, 2, \dots, n-1$ , which are nulls of the Chebyshev polynomials of the second kind. After substituting the unknown function  $\tilde{W}(t)$  with the Lagrange interpolation polynomial  $P_{n-2}(t)$  of order  $n-2$ , we have

$$\frac{1}{\pi} \int_{-1}^{+1} \frac{P_{n-2}(t)}{(t-t_0)^2} \sqrt{1-t^2} dt = \frac{1}{n} \sum_{\substack{j=1 \\ j \neq s}}^{n-1} P_{n-2}(t_{0j}^n) \frac{(1-t_{0j}^n)(1-(-1)^{j+s})}{(t_{0j}^n - t_0)^2} - n \frac{P_{n-2}(t_0)}{2} \quad (12)$$

$$\frac{1}{\pi} \int_{-1}^{+1} P_{n-2}(t) \ln |t - t_0| \sqrt{1-t^2} dt = \sum_{j=1}^{n-1} P_{n-2}(t_{0j}^n) \frac{(t_{0j}^n)^2 - 1}{n} \cdot \left[ \ln 2 + \sum_{k=1}^{n-1} \frac{T_k(t_{0j}^n) T_k(t_0)}{2^{-1}k} + \frac{(-1)^j}{n} T_n(t_0) \right] \quad (13)$$

$$\int_{-1}^{+1} P_{n-2}(t) \sqrt{1-t^2} dt = \frac{\pi}{n} \sum_{j=1}^{n-1} P_{n-2}(t_{0j}^n) (1 - t_{0j}^n)^2. \quad (14)$$

As a result, we obtain two decoupled matrix equations,

$$\sum_{j=1}^m V(\tau_j^m) (\alpha_{sj} + 4\delta_{sj} Q \kappa^{-1}) = g(\tau_s^m, \kappa), \quad s = \overline{1, m} \quad (15)$$

$$\sum_{j=1}^{n-1} \tilde{W}(t_{0j}^n) (\xi_{sj} + 4\delta_{js} R \sqrt{1-t_{0s}^n}) = f(t_{0s}^n, \kappa), \quad s = \overline{1, n-1}. \quad (16)$$

Here,  $V(\tau_s^m)$  and  $\tilde{W}(t_{0s}^n)$  are the unknown values of the surface current functions in the Simpson and Chebyshev nodes, respectively, and  $g(t, \kappa), f(t, \kappa)$  are smooth functions are the right-hand parts of IEs (7) and (8) in the same nodes.

We do not write here the coefficients  $\alpha_{sj}$  as they are easily derived using the classical Simpson quadratures [28] however

$$\xi_{sj} = \frac{(1-t_{0j}^n)^2}{n} \left\{ -i\kappa \left[ \ln 2 + 2 \sum_{l=1}^{n-1} \frac{1}{l} T_l(t_{0j}^n) T_l(t_{0s}^n) + (-1)^j \frac{1}{n} T_n(t_{0s}^n) \right] + \frac{4}{\kappa} \sum_{l=1}^{n-1} l U_{l-1}(t_{0j}^n) U_{l-1}(t_{0s}^n) + \pi N_0(t_{0j}^n, t_{0s}^n) \right\}. \quad (17)$$

Note that  $T_l(t), U_l(t)$  are the Chebyshev polynomials of the 1st and 2nd kind, respectively. On solving the matrix equations

we obtain approximate solutions to our SIEs in the form of interpolation polynomials for the unknown surface currents. The quadrature formulas ensure rapid convergence of the approximate solutions to the accurate ones (for the proof, see [18]–[23]) if  $m \rightarrow \infty$  and  $n \rightarrow \infty$ , respectively.

## B. Scattering Characteristics

Using the large-argument asymptotics for the Hankel functions in the kernels of (4), the scattered field in the far zone can be represented as  $u_{sc}(\vec{r}) \sim (2/i\pi k r)^{1/2} e^{ikr} \Phi(\varphi)$ , where  $\Phi(\varphi)$  is the scattering pattern. It is found as

$$\Phi(\varphi) = (i\kappa/4) \cdot \int_{-1}^1 \left[ V(t) - \frac{i}{2} \sin \varphi \sqrt{1-t^2} \tilde{W}(t) \right] e^{-i\kappa \cos \varphi} dt. \quad (18)$$

The total and backward scattering cross sections (TSCS and BSCS) (the latter quantity is also known as monostatic radar cross-section) characterize the total scattered power and that reflected back to the source, respectively

$$\sigma_{sc} = \left( \frac{2}{\pi k} \right) \int_0^{2\pi} |\Phi(\varphi)|^2 d\varphi, \quad \sigma_b = \frac{4|\Phi(\beta)|^2}{k}. \quad (19)$$

If the strip material is lossy, the heating losses are characterized by the absorption cross-section (ACS)

$$\sigma_{abs} = \int_{-d/2}^{d/2} [\text{Re } R |W(x)|^2 + \text{Re } Q |V(x)|^2] dx \quad (20)$$

that is linked to TSCS by the optical theorem

$$\sigma_{sc} + \sigma_{abs} = -4k^{-1} \text{Re} \Phi(\beta + \pi). \quad (21)$$

## IV. NUMERICAL RESULTS AND DISCUSSION

### A. Convergence

To see the actual rate of convergence, we computed the root-mean-square deviations of the norms of the surface current functions,  $\eta_V = \int_0^1 |V(t)|^2 dt$  and  $\eta_W = \int_{-1}^1 |\tilde{W}(t)|^2 \sqrt{1-t^2} dt$ , versus the matrix orders  $m, n$

$$e = \log \left| \frac{\eta_V^{m(n)}}{\eta_V^{2m(2n)}} - 1 \right|. \quad (22)$$

The plots in Fig. 2 demonstrate fast decrement of error in the H-wave case if the size of the quadrature formulas increases (the errors in the scattering cross-sections decay even faster).

### B. H-Case: Validation

To validate our algorithm, in Fig. 3, we present the normalized-frequency dependences of TSCS and BSCS for three strips illuminated by the normally incident H-wave.

Note that the cross sections are normalized by their high-frequency limits for a PEC strip under broadside illumination, that is by  $2d$  and  $k d^2$ , respectively. The PEC-strip results are presented with solid curves and show perfect agreement with the data known from the published papers and reference books (see [29]–[31]). Two other sets of curves are for the heavy-lossy dielectric strips. Note that the curves for the most lossy strip are very close to the PEC-strip curves. This is expected as, if  $|\varepsilon_r| \rightarrow \infty$ , then  $R \rightarrow 0$  and  $|Q| \rightarrow \infty$ .

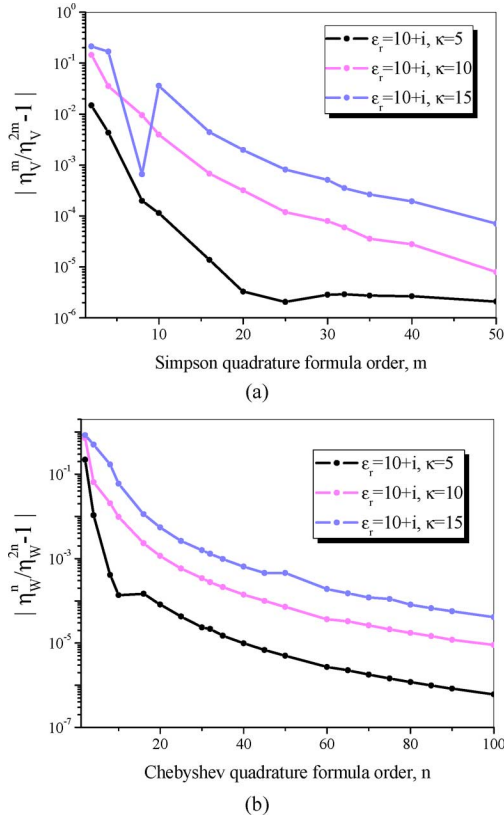


Fig. 2. The computation errors as a function of the quadrature orders,  $m$  and  $n$ , for the strips with  $\varepsilon_r = 10 + i$  and different values of  $\kappa$  ( $\beta = \pi/2$ ).

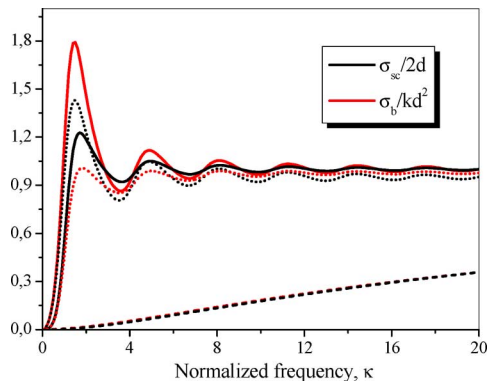


Fig. 3. Normalized TSCS and BSCS as a function of  $\kappa$  for the scattering of a normally incident ( $\beta = \pi/2$ ) H-wave by the PEC strip (solid) and by the lossy dielectric strips with  $\varepsilon_r = 1 + 30i$  (dashed) and  $\varepsilon_r = 1 + 3000i$  (dotted);  $h = d/400$ ,  $m = n = 100$ .

In Fig. 4, TSCS (a) and BSCS (b) are presented as a function of the incidence angle for the three dielectric strips and a PEC strip of the normalized width  $\kappa = 10$ .

As one can see, the curves corresponding to the densest strip nicely coincide with the PEC-strip curves for all angles of incidence except for  $\beta = 0$  where the latter curves go to zero.

Additional validation comes from the fact that in all cases the optical theorem (21) was satisfied with minimum 7 digits. We do not make comparison here with MoM computations because this has been already highlighted in [22], [23].

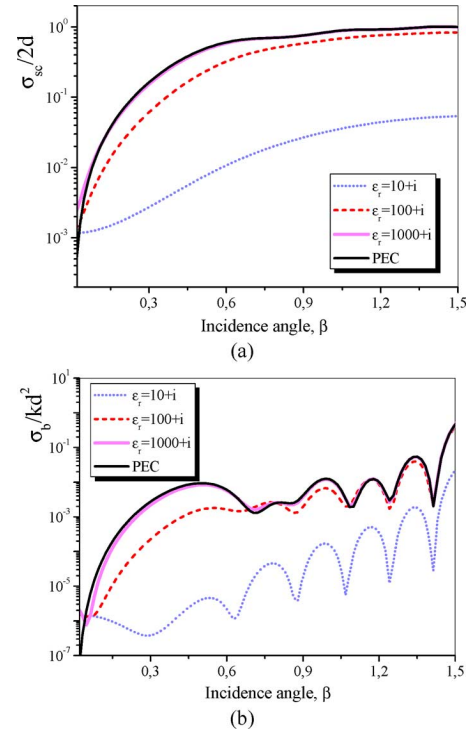


Fig. 4. Normalized TSCS (a) and BSCS (b) as a function of the H-wave incidence angle for the strip with  $\kappa = 10$ ; other parameters are as in Fig. 3.

### C. H-Case: Transversal Resonance

As mentioned above, the material strip model that is based on the GBC (1), (2) and resistivity formulas (3) takes into account the thickness of the strip even if it is larger than the wavelength in the strip material. Therefore it is interesting to analyze the scattering by the thin strips of varying width made of the dielectrics with relatively large real parts.

In Figs. 5 and 6, we present the frequency scans of the normalized cross-sections for  $h = d/400$ , under the normal and inclined incidences, respectively. Note that the permittivity of  $\varepsilon_r = 10 + i$  approximately corresponds to dry wood or paper at microwave frequencies. The “paper” strip scattering characteristics remain small and vary monotonically in the whole studied range. Another value taken here,  $\varepsilon_r = 1000 + i$ , is less usual however can be associated with one of the novel colossal-permittivity materials, see [32].

For such a strip, a single resonance appears around  $\kappa \approx 20$ . This is the frequency at which the infinite material slab is almost transparent for a normally incident plane wave as its thickness is a half-wavelength in the material ( $kh|\varepsilon_r|^{1/2} \approx \pi$ ).

Therefore this is a transversal resonance of infinite slab. For a finite strip, satisfaction of the same condition leads to the drop in BSCS at the normal incidence (Fig. 5(a)) and to the disappearance of the specular-scattering lobes in the in-resonance far-field patterns. Visualization of the in-resonance total near-field patterns shows that the central part of the strip remains transparent and the shadows are produced only by the strip edges—see Figs. 5(b) and 6(b). In this resonance, ACS displays maximum for any incidence angle.

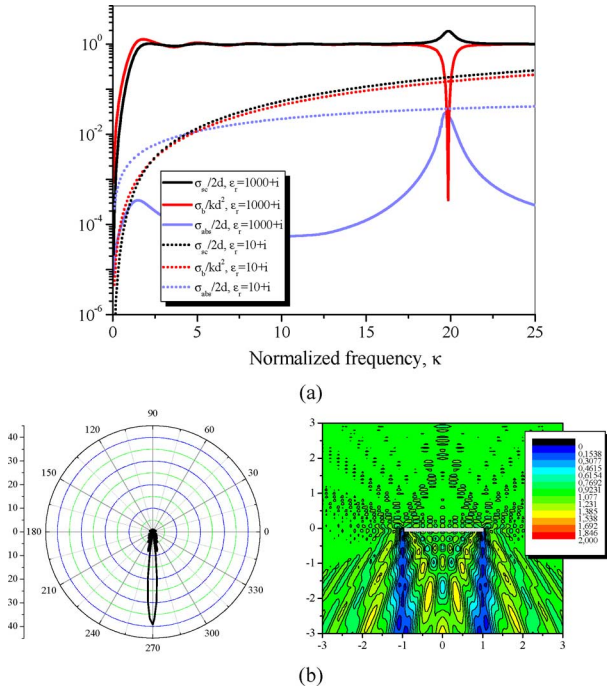


Fig. 5. Normalized TSCS, BSCS and ACS (a) as a function of  $\kappa$  for the normally incident H-wave ( $\beta = \pi/2$ ) scattering by thin dielectric strips with  $\epsilon_r = 10 + i$  (dotted curves) and  $\epsilon_r = 1000 + i$  (solid curves); the scattered far-field and the total near-field patterns at  $\kappa = 19.85$  (b);  $m = n = 100$ .

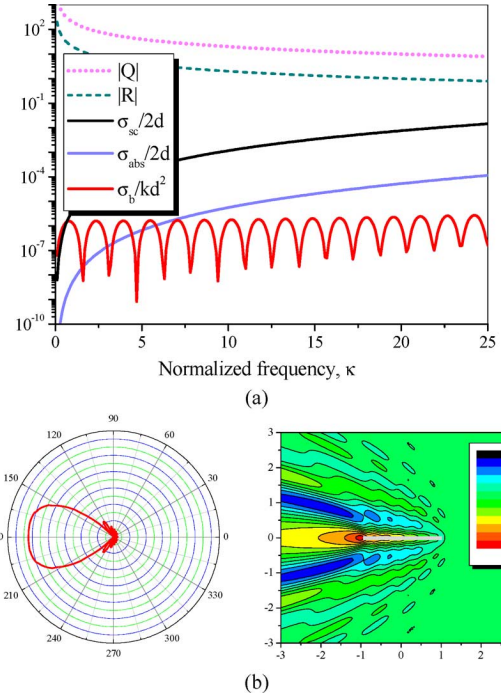


Fig. 7. Normalized TSCS and BSCS and relative resistivities  $|R|$  and  $|Q|$  as a function of  $\kappa$  (a), and scattered far-field and total near-field patterns for  $\kappa = 10$  (b) for the scattering by a dielectric strip with  $\epsilon_r = 10 + i$  and  $h = d/100$ ;  $m = n = 100$  under the edge-on incidence of H-wave.

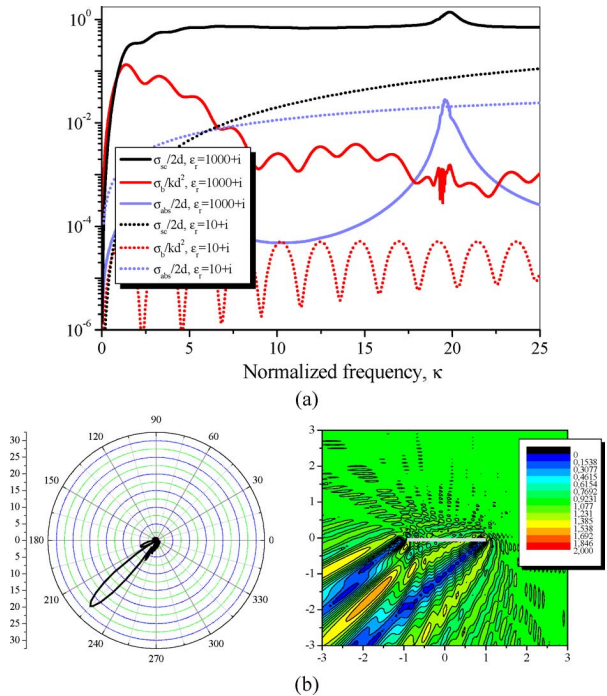


Fig. 6. The same as in Fig. 6 for the inclined ( $\beta = \pi/4$ ) incidence of H-wave (a); the field patterns at  $\kappa = 19.85$  and  $\epsilon_r = 1000 + i$  (b).

If the incidence is inclined then the BSCS plot displays a sequence of periodic low-intensity oscillations (Fig. 6(a)). Their nature will be discussed in the next sub-section.

#### D. H-Case: Edge-on Incidence

Flat zero-thickness PEC strips are invisible at the edge-on incidence of the H-polarized plane wave. In contrast, material strips remain visible even at the edge-on incidence as they still scatter and absorb the H-wave. Note that in this case  $\beta = 0$  and hence  $W \equiv 0$  as follows from (6).

In Figs. 7(a) and 8(a), we present the dependences of the normalized TSCS, ACS and BSCS on the normalized strip width, for two dielectric strips with  $\epsilon_r = 10 + i$  and  $\epsilon_r = 1000 + i$  under the edge-on illumination, respectively.

Note that BSCS remains small however displays a sequence of low-level periodic oscillations with period of  $\pi/2$  that corresponds to the increment of the strip width by  $\lambda/2$ . These maxima and minima are explained by the in-phase and anti-phase contributions of the leading and trailing edges of the strip to the backscattered field. They are not connected to the natural modes of the strip as open resonator.

Such explanation is proven by the fact that the locations of the minima and maxima do not depend on the value of  $\epsilon_r$ .

The “paper” strip TSCS and ACS also remain small and vary monotonically in the whole studied frequency range. However the denser strip characteristics (Fig. 8(a)) demonstrate the transversal resonance around  $\kappa = 19$  that has been discussed in the previous section. The far-field scattering patterns and the total near-field patterns in Figs. 7(b) and 8(b) reveal that, in either case, the field is dominated by the forward scattering and the shadow, respectively.

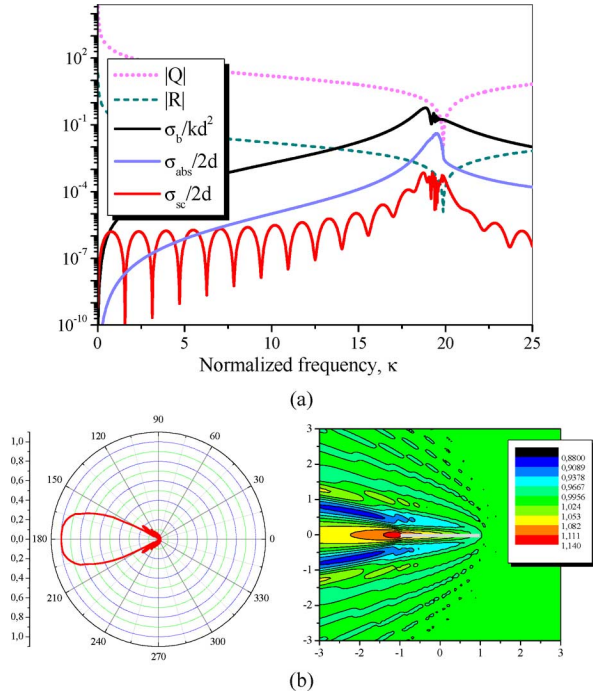


Fig. 8. The same as in Fig. 7 for  $\epsilon_r = 1000 + i$  and  $\kappa = 18.85$  in (b).

### E. E-Polarization Case: Longitudinal Resonances

The alternative case of the E-polarized plane wave scattering is considered similarly to the H-case. It reduces to two IEs like (7) and (8) however with  $R$  and  $Q$  exchanging their places. Formally small difference, it entails major modifications in the behavior of the cross sections.

In Fig. 9, presented are the normalized TSCS, BSCS and ACS values as a function of the frequency parameter  $\kappa$  for E-polarized plane wave incident normally and in the edge-on manner. The strip has the permittivity  $\epsilon_r = 100 + 0.1i$  and thickness  $h = d/400$ . Unlike the H-wave case, here one can see many sharp resonances in the scattering and absorption. These resonances correspond to the natural Fabry-Perot-like modes  $E_{p0}$  of a thin dielectric strip where  $p = 1, 2, 3, 4 \dots$  and hence are longitudinal resonances.

As it is suggested by the effective refractive index model of a thin dielectric layer [33], the approximate characteristic equation for such resonances is  $\cos(2\kappa \text{Re}(\alpha_{eff}^E)) \approx 0$ , where  $\alpha_{eff}^H = [1 - 1/(4Q^2)]^{1/2}$  as follows from (1) and (2). This quantity is a function of the frequency and layer material; it appears as the normalized propagation coefficient of the E-polarized principal guided wave ( $TM_0$ ) of the infinite layer.

In Fig. 10, we show the dependences of the real and imaginary parts of  $\alpha_{eff}^E$  on  $\kappa$  for the corresponding dielectric layer. One can verify that the roots of the mentioned equation, marked in Fig. 9 as stars above the  $\kappa$  axis, are indeed close to the resonances.

Note that in the case of the H-polarization the corresponding effective refractive index of a thin strip is found to be  $\alpha_{eff}^H = [1 - 1/(4Q^2)]^{1/2}$ . This value is much closer to 1 than  $\alpha_{eff}^E$  (even if  $|\epsilon| \approx 1000$ ) and therefore no associated sharp longitudinal resonances are visible in Figs. 6 and 8.

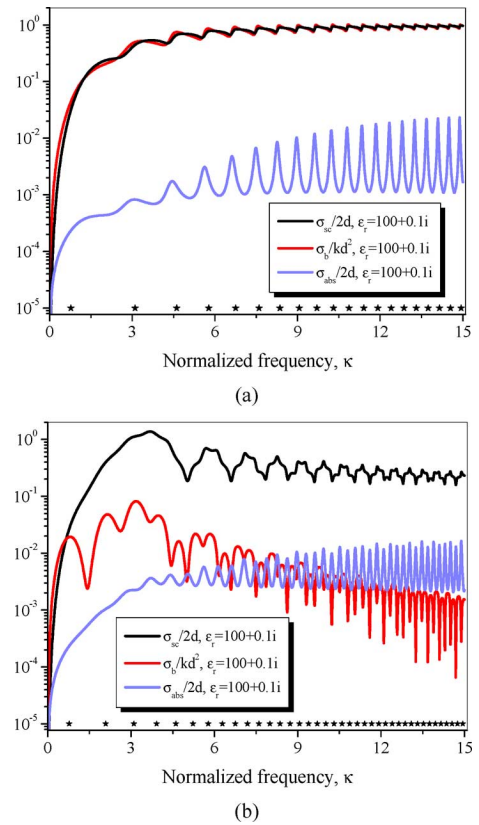


Fig. 9. Normalized TSCS, BSCS and ACS as a function of  $\kappa$  for the scattering by the strip with  $\epsilon_r = 100 + 0.1i$  for the normal (a) and edge-on (b) incidence of E-wave; other parameters are  $h = d/100$ , and  $m = n = 150$ .

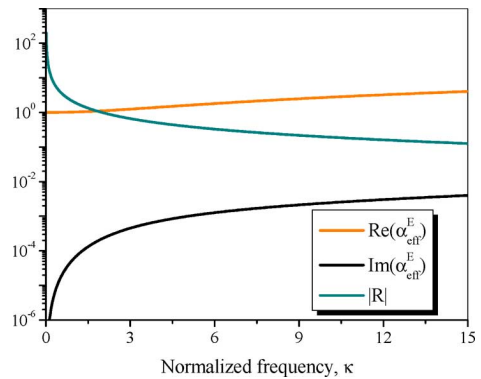


Fig. 10. The real and imaginary parts of  $\alpha_{eff}^E$  and relative resistivity  $|R|$  as a function of  $\kappa$  for the strip with  $\epsilon_r = 100 + 0.1i$ .

Finally, Fig. 11 presents the field patterns in four resonances for the normally-incident plane E-wave scattering (because of the symmetry of excitation only the longitudinal strip modes  $E_{p0}$  corresponding to odd values of  $p$  are excited). As one can see, the in-resonance far fields display sizable scattering in the strip plane, in addition to the intensive shadow and specular scattering.

Note that these results can be viewed as partial justification of the empiric effective refractive index model of a thin dielectric strip that enables one to reduce the dimensionality when searching for the frequencies of longitudinal resonances.

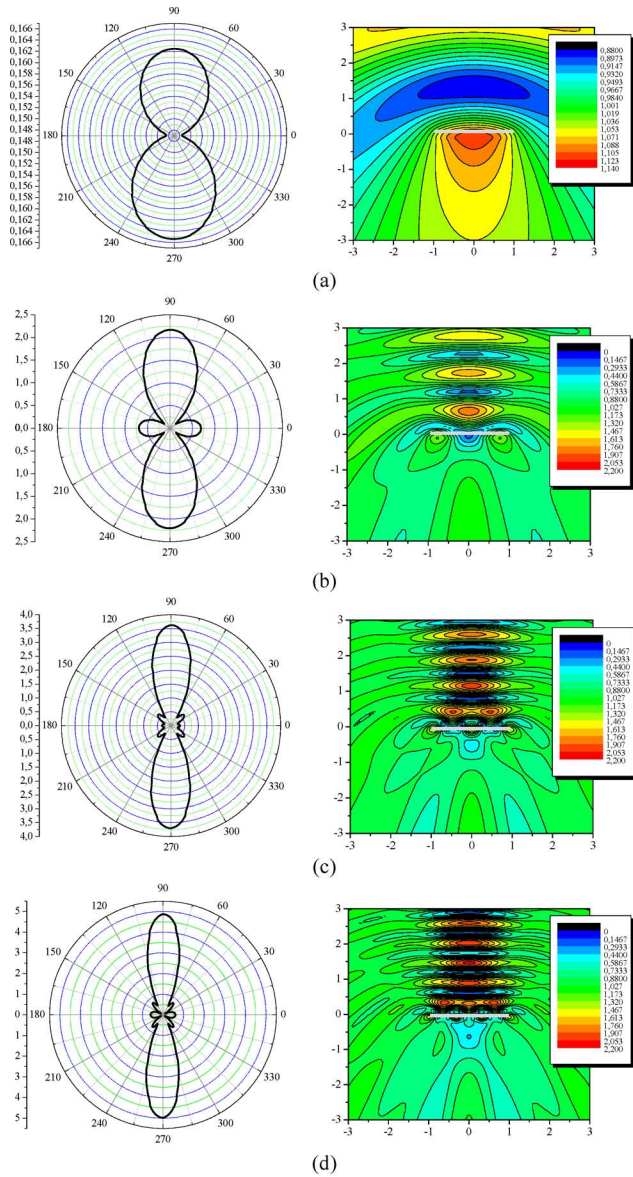


Fig. 11. The field patterns in the  $E_{p0}$  mode resonances ( $p = 1, 3, 5, 7$ ) for the normal incidence of plane wave on the strip with  $\varepsilon_r = 100 + 0.1i$  and  $h = d/400$  at  $\kappa = 0.77$  (a),  $\kappa = 3.08$  (b),  $\kappa = 4.45$  (c) and  $\kappa = 5.63$  (d);  $m = n = 150$ .

## V. CONCLUSIONS

We have presented an efficient and accurate method to analyze the scattering by a thin flat magneto-dielectric strip in free space illuminated by a plane electromagnetic wave. This method of numerical modeling is based on two decoupled log-singular and hyper-singular IEs for the electric and magnetic surface currents on the strip and uses their direct discretization with the aid of the special quadrature formulas of interpolation type. In contrast to the conventional moment method with local basis functions it has guaranteed convergence and controlled accuracy of computations. Besides, it is simpler in implementation than the analytical regularization methods.

We have presented the numerical results for the H- and E-polarization cases and investigated the scattering and absorption

properties of the lossy dielectric strips, including the field behavior in the far and near zones. In the case of the H-polarization, a transversal resonance has been studied. This resonance results in good transparency of the strip at the normal incidence of plane wave, so that only the edges contribute to the scattering. We have also given special consideration to the edge-on incidence case because thin magneto-dielectric strips remain visible in this case even under the H-wave illumination, unlike the PEC strips.

In the case of the E-polarization, we have demonstrated the sequence of resonances in the scattering and absorption. They are explained as the longitudinal Fabry-Perot resonances of the natural wave of the corresponding dielectric layer traveling from one end of the thin strip to another. Such an effect is absent in the H-polarization case because of much smaller propagation constant of the corresponding natural wave of the same dielectric layer.

Thus we have built a relatively universal mathematical model that enables one to investigate a wide class of the flat material striplike scatterers in the resonance range.

## ACKNOWLEDGMENT

The authors are grateful to Dr. E.I. Smotrova and Dr. V.S. Bulygin for many helpful discussions and to the anonymous reviewer for valuable comments.

## REFERENCES

- [1] D. Colton and R. Kress, *Integral Equations Methods in Scattering Theory*. New York: Wiley, 1983.
- [2] G. A. Grinberg, "Boundary conditions for the electromagnetic field in the presence of thin metallic shells," (in Russian) *Radio Engrg. Electron.*, vol. 26, no. 12, pp. 2493–2499, 1981.
- [3] G. Bouchitté, "Analyse limite de la diffraction d'ondes électromagnétiques par une structure mince," *C.R. Acad. Paris*, ser. II, vol. 311, pp. 51–56, 1990.
- [4] E. Bleszynski, M. Bleszynski, and T. Jaroszewicz, "Surface-integral equations for electromagnetic scattering from impenetrable and penetrable sheets," *IEEE Antennas Propag. Mag.*, vol. 36, no. 6, pp. 14–25, 1993.
- [5] T. B. A. Senior, "Backscattering from resistive strips," *IEEE Trans. Antennas Propag.*, vol. 27, no. 6, pp. 808–813, 1979.
- [6] S. Dowerah and A. Chacrabarty, "Extinction cross section of a dielectric strip," *IEEE Trans. Antennas Propag.*, vol. 38, no. 5, pp. 696–706, 1988.
- [7] T. B. A. Senior and J. L. Volakis, "Sheet simulation of a thin dielectric layer," *Radio Sci.*, vol. 22, no. 7, pp. 1261–1272, 1987.
- [8] T. B. A. Senior and J. L. Volakis, *Approximate Boundary Conditions in Electromagnetics*. London: The IEE Press, 1995.
- [9] R. C. Hall and R. Mittra, "Scattering from a periodic array of resistive strips," *IEEE Trans. Antennas Propag.*, vol. 33, no. 9, pp. 1009–1011, 1985.
- [10] R. Petit and G. Tayeb, "Theoretical and numerical study of gratings consisting of periodic arrays of thin and lossy strips," *J. Opt. Soc. Amer.*, vol. 7, no. 9, pt. A, pp. 1686–1692, 1990.
- [11] Z. S. Agranovich, V. A. Marchenko, and V. P. Shestopalov, "Diffraction of a plane electromagnetic wave from plane metallic lattices," *Soviet Phys. Tech. Phys.*, vol. 7, pp. 277–286, 1962.
- [12] A. Matsushima and T. Itakura, "Singular integral equation approach to plane wave diffraction by an infinite strip grating at oblique incidence," *J. Electromagn. Waves Applcat.*, vol. 4, no. 6, pp. 505–519, 1990.
- [13] A. I. Nosich, "Green's function – Dual series approach in wave scattering from combined resonant scatterers," in *Analytical and Numerical Methods in Electromagnetic Wave Theory*, M. Hashimoto, M. Idemen, and O. A. Tretyakov, Eds. Tokyo: Science House, 1993, ch. 9, pp. 419–469.

- [14] A. I. Nosich, "Method of analytical regularization in wave-scattering and eigenvalue problems: Foundations and review of solutions," *IEEE Antennas Propag. Mag.*, vol. 42, no. 3, pp. 34–49, 1999.
- [15] A. I. Nosich, Y. Okuno, and T. Shiraishi, "Scattering and absorption of E- and H-polarized plane waves by a circularly curved resistive strip," *Radio Sci.*, vol. 31, no. 6, pp. 1733–1742, 1996.
- [16] T. L. Zinenko, A. I. Nosich, and Y. Okuno, "Plane wave scattering and absorption by resistive-strip and dielectric-strip periodic gratings," *IEEE Trans. Antennas Propag.*, vol. 46, no. 10, pp. 1498–1505, 1998.
- [17] T. L. Zinenko and A. I. Nosich, "Plane wave scattering and absorption by flat gratings of impedance strips," *IEEE Trans. Antennas Propag.*, vol. 54, no. 7, pp. 2088–2095, 2006.
- [18] Z. T. Nazarchuk, *Numerical Investigation of Wave Diffraction by Cylindrical Structures* (in Russian). Kyiv: Naukova Dumka, 1989.
- [19] Z. Nazarchuk and K. Kobayashi, "Mathematical modelling of electromagnetic scattering from a thin penetrable target," *Progr. Electromagn. Res.*, vol. 55, pp. 95–116, 2005.
- [20] Y. V. Gandel, *Introduction to the Methods of Computations of Singular and Hyper-Singular Integrals*. Kharkiv: KhNU Press, 2001.
- [21] J. Tsalamengas, "Exponentially converging Nystrom's methods for systems of SIEs with applications to open/closed strip or slot-loaded 2-D structures," *IEEE Trans. Antennas Propag.*, vol. 54, no. 5, pp. 1549–1558, 2006.
- [22] J. Tsalamengas, "Exponentially converging Nystrom methods in scattering from infinite curved smooth strips—Pt. 1: TM case," *IEEE Trans. Antennas Propag.*, vol. 58, no. 10, pp. 3265–3274, 2010.
- [23] J. Tsalamengas, "Exponentially converging Nystrom methods in scattering from infinite curved smooth strips—Pt. 2: TE case," *IEEE Trans. Antennas Propag.*, vol. 58, no. 10, pp. 3275–3281, 2010.
- [24] A. A. Nosich and Y. V. Gandel, "Numerical analysis of quasi-optical multireflector antennas in 2-D with the method of discrete singularities," *IEEE Trans. Antennas Propag.*, vol. 55, no. 2, pp. 399–406, 2007.
- [25] A. A. Nosich and Y. V. Gandel, "Role of edge illumination in the mm-range elliptic reflector beam waveguide performance," in *Proc. Eur. Microwave Conf. (EuMC-07)*, Munich, 2007, pp. 376–379.
- [26] A. A. Nosich, Y. V. Gandel, A. Matsushima, and R. Sauleau, "Collimation and focusing of wave beams with metal-plate lens antennas analyzed using Nystrom-type MDS algorithm," presented at the Proc. IEEEAP-S Int. Symp. (APS-08), San Diego, 2008, session 237.10.
- [27] A. A. Nosich, R. Sauleau, and Y. V. Gandel, "Classical ADE and PACO 2-D omnidirectional dual-reflector antennas simulated in 2-D using a Nystrom-type MDS algorithm," in *Proc. Eur. Microwave Conf. (EuMC-09)*, Rome, 2009, pp. 858–861.
- [28] M. Abramowitz and I. A. Stegun, Eds., *Handbook of Mathematical Functions*. New York, Dover, 1979.
- [29] J. J. Bowman, T. B. A. Senior, and P. L. E. Uslenghi, *Electromagnetic and Acoustic Scattering by Simple Shapes*. Amsterdam: North-Holland, 1969.
- [30] G. T. Ruck, Ed., *Radar Cross-Section Handbook*. New York, Plenum-Press, 1970.
- [31] H. C. van de Hulst, *Light Scattering by Small Particles*. New York: Dover Publications, 1981.
- [32] S. Krohns *et al.*, "Colossal dielectric constant up to gigahertz at room temperature," *Appl. Phys. Lett.*, vol. 94, no. 12, pp. 2903–2905, 2009.
- [33] E. I. Smotrova, A. I. Nosich, T. Benson, and P. Sewell, "Cold-cavity thresholds of microdisks with uniform and non-uniform gain: Quasi-3D modeling with accurate 2D analysis," *IEEE J. Sel. Topics Quant. Electron.*, vol. 11, no. 5, pp. 1135–1142, 2005.



**Olga V. Shapoval** (S'10) was born in Nikopol, Ukraine, in 1987. She received the M.S. degree in applied mathematics (with honors) from Kharkiv National University, in 2009. She is currently working toward the Ph.D. degree at the National Academy of Science of Ukraine, Kharkiv.

Her current research interests are in the scattering problems by striplike structures, efficient mathematical and numerical solution techniques, and singular and hyper-singular integral equations.

Ms. Shapoval was a recipient of the 2010 URSI Young Scientist Award for attending the Asia-Pacific Radio Science Conference in Toyama and the Doctoral Research Award from the IEEE Antennas and Propagation Society.



**Ronan Sauleau** (M'04–SM'06) was born in Rennes, France, in 1972. He received the Electronic Engineering and Radiocommunications degree and the French DEA degree in electronics from the Institut National des Sciences Appliquées (INSA), Rennes, France, in 1995, the Aggregation degree from Ecole Normale Supérieure de Cachan, France, in 1996, and the Doctoral degree in signal processing and telecommunications from the Institut d'Électronique et Télécommunications de Rennes (IETR), University of Rennes 1, in 1999.

Since 1999, he has been on the staff of IETR and was elected Professor in 2009. His main fields of interest are millimeter wave printed antennas, focusing devices, and periodic structures including electromagnetic bandgap materials and metamaterials.

Dr. Sauleau received the 2004 ISAP Conference Young Scientist Travel Grant and the first Young Researcher Prize in Brittany, France, in 2001 for his work on gain-enhanced Fabry-Perot antennas. In 2007, he was elected a Junior Member of the Institut Universitaire de France.



**Alexander I. Nosich** (M'94–SM'95–F'04) was born in 1953 in Kharkiv, Ukraine. He received the M.S., Ph.D., and D.Sc. degrees in radio physics from the Kharkiv National University, Ukraine, in 1975, 1979, and 1990, respectively.

Since 1979, he has been with the Institute of Radio Physics and Electronics, National Academy of Science of Ukraine, Kharkiv, where he is currently Professor and Principal Scientist heading the Laboratory of Micro and Nano-Optics. Since 1992, he has held a number of guest fellowship and professorship in the

EU, Japan, Singapore, and Turkey. His research interests include the method of analytical regularization, propagation and scattering of waves in open waveguides, simulation of the semiconductor lasers and antennas, and the history of microwaves.

Prof. Nosich was one of the initiators and technical committee chairman of the international conference series on Mathematical Methods in Electromagnetic Theory (MMET). In 1995, he organized the IEEE AP-S East Ukraine Chapter, the first one in the former USSR. Currently, he represents Ukraine, Georgia, and Moldova in the European Association on Antennas and Propagation.